Valence-state transition in $SrMn_{1-x}Mo_xO_3$ ($0 \leq x \leq 0.5$) investigated by soft x-ray absorption spectroscopy

Jieun Lee, Bongjae Kim, B. H. Kim, and B. I. Min
Department of Physics, Pohang University of Science and Technology, Pohang 790-784, Korea

S. Kolesnik, O. Chmaissem, J. Mais, and B. Dabrowski
Department of Physics, Northern Illinois University, DeKalb, Illinois 600115, USA

H. J. Shin
Pohang Accelerator Laboratory, Pohang University of Science and Technology, Pohang 790-784, Korea

D. H. Kim, H. J. Lee, and J.-S. Kang*
Department of Physics, The Catholic University of Korea (CUK), Bucheon 420-743, Korea
(Received 11 August 2009; published 13 November 2009)

The electronic structures of perovskite $SrMn_{1-x}Mo_xO_3$ ($0 \leq x \leq 0.5$) have been investigated by employing soft x-ray absorption spectroscopy (XAS). Mn $2p$ XAS shows the systematic change in the valence states of Mn ions in $SrMn_{1-x}Mo_xO_3$ due to the substitution of hexavalent $Mo^{6+}(4d^0)$ ions. With increasing x, the valence states and the spin configurations of Mn ions change from high-spin (HS) Mn^{4+} for $x=0$, to HS $Mn^{3+}(t_{2g}^3\uparrow e_g^1\uparrow)$ for $x=0.3$, and HS $Mn^{2+}(t_{2g}^3\uparrow e_g^2\uparrow)$ for $x=0.5$. The measured Mn $2p$ XAS spectra are described well with the configuration interaction (CI) cluster model, including the Jahn-Teller distortion effect for Mn^{3+} ions. The combination of the findings of Mn $2p$ XAS and the CI calculations provides the complete picture of the electronic structures of $SrMn_{1-x}Mo_xO_3$ for $0 \leq x \leq 0.5$.

DOI: 10.1103/PhysRevB.80.205112 PACS number(s): 78.70.Dm, 74.25.Jb, 71.20.−b, 71.30.+h

I. INTRODUCTION

$SrMnO_3$ is a parent compound of the widely studied mixed-valent perovskite manganites (ABO_3). When the divalent A ion is replaced by a trivalent rare-earth, a variety of changes has been observed[1] in crystallographic, electronic, and magnetic properties. Likewise, the B-site doping with different transition-metal (T) elements has attracted attention due to the observed large room-temperature magnetoresistance (MR) in double-perovskites.[2] Several experimental and theoretical studies[3–5] on cubic $SrMnO_3$ have revealed that $SrMnO_3$ is a G-type antiferromagnetic (AFM) insulator ($T_N \sim 233$ K) with the Mn^{4+} valence state. On the other hand, double perovskite Sr_2MnMoO_6 is known to be a monoclinically distorted AFM insulator ($T_N \sim 12$ K),[6] but the valence states of the B-site ions have been controversial between ($Mn^{2+}-Mo^{6+}$) (Refs. 7 and 8) and ($Mn^{3+}-Mo^{5+}$).[9] Therefore determining the valence states of Mn and Mo in Sr_2MnMoO_6 and confirming their expected change in $SrMn_{1-x}Mo_xO_3$ ($0 \leq x \leq 0.5$) in relation to the structural, electronic, and magnetic properties are worth of further investigation.

It was reported that the Mo substitution in $LaMnO_3$ induces ferromagnetism (FM), which originates from the double-exchange (DE) interaction between Mn^{3+} and Mn^{2+} ions.[10] Prior to that, Mo-doped $CaMnO_3$ ($T_N \sim 125$ K) captured much attention due to the creation of the colossal magnetoresistance (CMR) effect.[11,12] The advantage of Mo substitution for Mn is that a large variation in the Mn valence is possible due to the high valency of a Mo ion (Mo^{5+} or Mo^{6+}), while the structural disorder in the Mn lattice is relatively small. Nevertheless, for Mo-doped $SrMnO_3$, which is similar to $CaMnO_3$, no systematic studies have been reported yet. The end member $SrMoO_3$ is a paramagnetic metal.[13] According to the previous study[13] on Mn-doped $SrMoO_3$ ($SrMo_{1-y}Mn_yO_3$: $0 \leq y \leq 0.2$), the metal-to-insulator transition occurs for $y \geq 0.03$, which is accompanied by the change in the magnetic property from the Pauli to Curie-Weiss paramagnetism for $y \geq 0.01$. Further, the increase in the lattice constant with Mn doping suggested the existence of Mn^{2+}, since the radius of Mn^{4+} (0.53 Å) is much smaller than those of Mo^{4+} (0.65 Å) and Mn^{2+} (0.67 Å).

In this work, we have investigated the electronic structures of $SrMn_{1-x}Mo_xO_3$ ($0 \leq x \leq 0.5$) by employing soft x-ray absorption spectroscopy (XAS), which is known to be a powerful experimental tool for studying the valence and spin states of T ions in solids. This work shows that XAS provides the experimental evidence for the systematic changes in the electronic structure and the valence states in $SrMn_{1-x}Mo_xO_3$. The configuration interaction (CI) cluster calculations confirm these experimental findings theoretically.

II. EXPERIMENTAL DETAILS

High-quality polycrystalline samples of $SrMn_{1-x}Mo_xO_3$ ($0 \leq x \leq 0.5$) were synthesized by standard solid-state reaction methods. Single-phase cubic perovskite $SrMnO_3$ and lightly Mo-substituted compositions were obtained by using a two-step synthesis method.[14] X-ray diffraction and neutron powder diffraction measurements showed that all the samples, employed in this work, have no impurity phase. The samples with $x=0$, 0.2, and 0.3 are single-phase cubic perovskites ($Pm\bar{3}m$) at room temperature. The sample with x

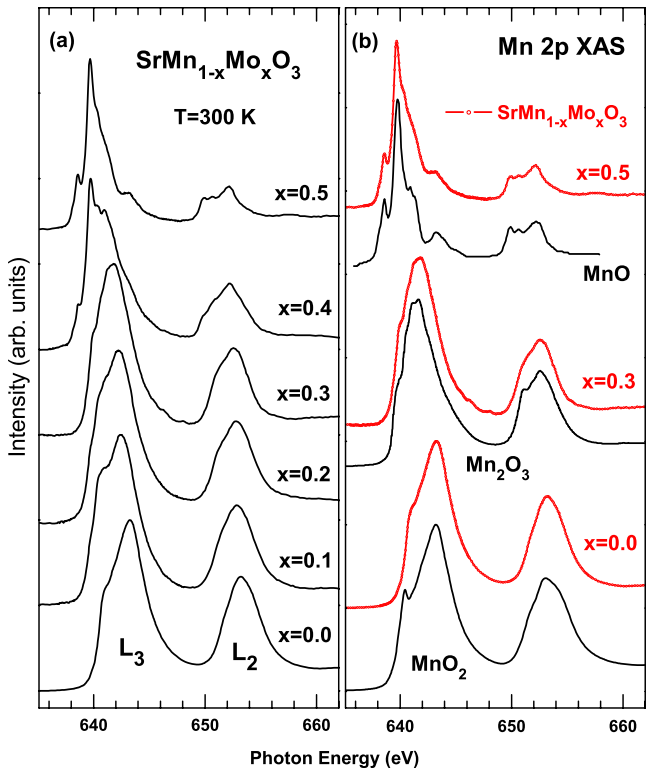

FIG. 1. (Color online) Comparison of the (a) Mn $2p$ XAS spectra of $SrMn_{1-x}Mo_xO_3$ $(0 \leq x \leq 0.5)$ with those of (b) MnO (Mn^{2+}), $Mn_2O_3(Mn^{3+})$, and $MnO_2(Mn^{4+})$.

$=0.1$ is single-phase tetragonal $(I4/mcm)$. The sample with $x=0.4$ is a mixture of cubic $Pm\bar{3}m$ and monoclinic $P21/n$ phases in the approximate ratio of 3:2. The sample with $x=0.5$ is a monoclinically distorted $(P21/n)$ single-phase double perovskite. All the samples were found to be insulators. XAS measurements were performed at the U7 beamline of the Pohang light source (PLS). The chamber pressure was better than 7×10^{-10} Torr. All the samples were cleaned *in situ* by repeated scrapings with a diamond file to remove the surface contamination. XAS spectra were obtained both at room temperature and at $T \sim 80$ K (Ref. 15) by employing the total electron yield (TEY) mode with the photon energy resolution of ~ 100 meV at $h\nu \approx 600$ eV. All the XAS spectra were normalized to the incident photon flux.

III. RESULTS AND DISCUSSION

Figure 1(a) shows the measured Mn $2p$ XAS spectra of $SrMn_{1-x}Mo_xO_3$ $(0 \leq x \leq 0.5)$. All the spectra are split into $L_3(2p_{3/2})$ and $L_2(2p_{1/2})$ parts due to the $2p$ core-hole spin-orbit coupling. With increasing x in $SrMn_{1-x}Mo_xO_3$, both the L_3 and L_2 edges shift gradually toward the lower energies and their spectral shapes change. T $2p$ XAS is highly sensitive to its valence state by reflecting the $2p$ core-hole final-state multiplets due to the interaction between the $2p$ hole and the $3d$ electrons, where the number of $3d$ electrons plays an important role. Therefore, the spectral change in the series of $SrMn_{1-x}Mo_xO_3$ suggests the gradual variation in the Mn valency.[16] By comparing these Mn $2p$ XAS spectra to those of various reference manganese oxides, as shown in Fig. 1(b), the valence states of Mn ions in $SrMn_{1-x}Mo_xO_3$ for different x can be identified. Figure 1(b) compares the measured Mn $2p$ XAS spectra of $SrMn_{1-x}Mo_xO_3$ for $x=0$, 0.3, 0.5 with those of $MnO_2(Mn^{4+})$ (Ref. 17) (bottom), $Mn_2O_3(Mn^{3+})$ (Ref. 18) (middle), and MnO (Mn^{2+}) (Ref. 19) (top), respectively. It is clearly shown that both the peak shifts and the lineshapes in $SrMn_{1-x}Mo_xO_3$ with increasing x agree well with those from MnO_2 to Mn_2O_3 and MnO. This comparison provides evidence that the formal valence states (v) of Mn ions in $SrMn_{1-x}Mo_xO_3$ decrease from $v \approx 4$ for $x=0$ to $v \approx 3$ for $x=0.3$ and $v \approx 2$ for $x=0.5$.

From the XAS investigation, the valence states of Mn in $SrMn_{1-x}Mo_xO_3$ are found to change gradually from being tetravalent $(Mn^{4+}:3d^3)$ to divalent $(Mn^{2+}:3d^5)$ through being trivalent $(Mn^{3+}:3d^4)$ via the substitution of Mo for Mn. In order to verify this change in the Mn valence state, we have analyzed the ground states of Mn ions in $SrMn_{1-x}Mo_xO_3$ by performing CI cluster calculations. The CI cluster calculation enables us to make a quantitative description of the spectral features and the ground states of Mn ions.

In the CI model with the octahedral (O_h) symmetry, the free-atomic multiplets due to the six oxygen (O^{2-}) environment in the perovskite structure are determined by the crystal field, which splits the energy levels of $3d$ orbitals, and the hybridization, which takes account of the covalency between T $3d$ and O $2p$ states.[20] The $2p$-$3d$ and $3d$-$3d$ Coulomb and exchange interactions are reduced, which is considered to account for the solid-state screening. In order to minimize the number of adjustable parameters, we have fixed the reduction rates for the Coulomb and exchange interactions to $\sim 80\%$ with a little margin. The hopping parameter strength, especially $V_{pd\sigma}$, was estimated from r_d and d_{M-O} by using the relation given by Harrison,[21,22] where r_d denotes the radial extent of the $3d$ orbital and d_{M-O} denotes the metal-oxygen distance. The value of $V_{pd\pi}$ is chosen to be a half of $V_{pd\sigma}$ as a usual practice. In this calculation, the difference between U_{pd} and U_{dd} is fixed to $\Delta U = |U_{pd}| - U_{dd} = 1-2$ eV (U_{pd}: the attractive $2p$-$3d$ Coulomb interaction, U_{dd}: the repulsive $3d$-$3d$ Coulomb interaction).[23] In this way, only few physical parameters are optimized to fit the experimental data: the crystal-field strengths of $10Dq$ and Δ_{JT}, and the charge-transfer energy Δ. Here, $10Dq$ corresponds to the energy separation between t_{2g} and e_g orbitals, Δ_{JT} represents the Jahn-Teller splitting under the D_{4h} tetragonal symmetry, and Δ corresponds to the energy needed to transfer one electron from the ligand band to the T $3d$ orbital. Finally, the calculated multiplets are broadened with the Lorentzian and Gaussian functions. The Lorentzian broadening, 2γ, describes the core-hole life time,[24] while the Gaussian broadening describes the instrumental resolution.

Figures 2(a)–2(c) compares the measured Mn $2p$ XAS spectra of $SrMn_{1-x}Mo_xO_3$ for $x=0$, $x=0.3$, and $x=0.5$ to the CI cluster calculations for $Mn^{4+}(O_h)$, Mn^{3+} (for both O_h and D_{4h} symmetries), and $Mn^{2+}(O_h)$ ions, respectively. This comparison reveals a good agreement between calculations and experiment. The parameters, which are determined from these fittings, are listed in Table I.

We first start our discussion on the fitting results for $x=0.5(Mn^{2+})$ in Fig. 2(c) because it is the simplest among the

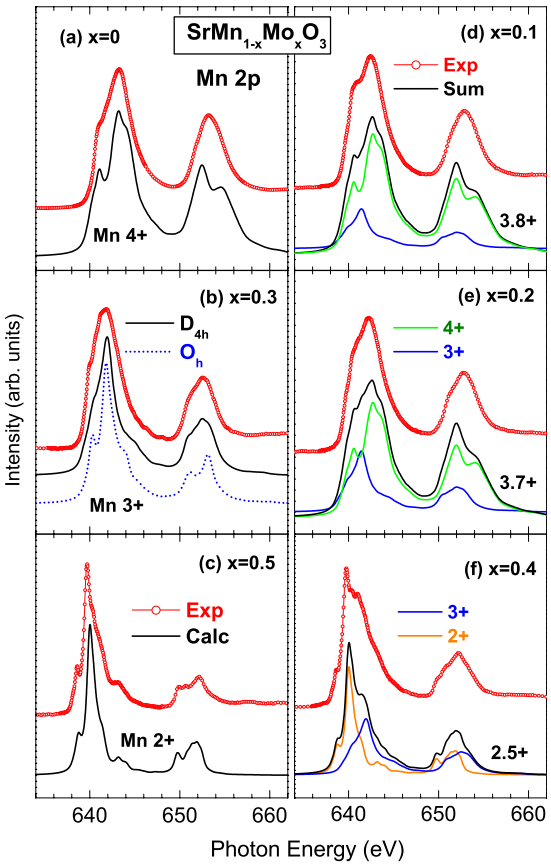

FIG. 2. (Color online) (a)–(c) Comparison of the measured Mn $2p$ XAS of $SrMn_{1-x}Mo_xO_3$ for $x=0$, $x=0.3$, and $x=0.5$ to the calculated Mn $2p$ XAS for $Mn^{4+}(O_h)$, Mn^{3+} (for both O_h and D_{4h}), and $Mn^{2+}(O_h)$ ions, respectively. (d)–(f) Comparison of the Mn $2p$ XAS spectra of $SrMn_{1-x}Mo_xO_3$ for $x=0.1$, $x=0.2$, and $x=0.4$ to the weighted sums of calculated Mn^{4+}, Mn^{3+}, and Mn^{2+}. See the text for the details.

fits shown in Fig. 2. The spin state of a Mn ion is determined by the relative strength between 10 Dq and J_{eff}, where J_{eff} represents the difference in the exchange energy, with respect to 10 Dq, between the high-spin (HS) and the low-spin (LS) configuration. J_{eff} can be estimated from the Stoner exchange splitting J, and $J_{eff}=3J$ for Mn^{2+}. The Stoner exchange splitting J is given as a linear combination of the Slater-Condon parameters[23] as $J=(F_2+F_4)/14$. For $x=0.5$, $J=0.8$ eV, and 10 Dq=0.9 eV (see Table I) yield $J_{eff}=2.4$ eV. So J_{eff} is larger than 10 Dq, resulting in the HS Mn^{2+} states for $x=0.5$.

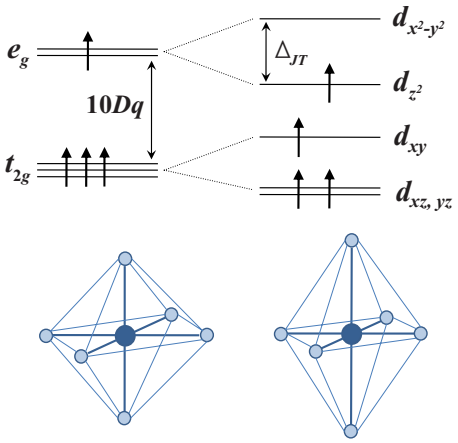

FIG. 3. (Color online) The Jahn-Teller effect for $Mn^{3+}(3d^4)$. The distortion of octahedral $(O_h)MnO_6$ (left) to tetragonal $(D_{4h})MnO_6$ (right) splits the t_{2g} and e_g states.

The Mn $2p$ XAS spectrum for $x=0.3$ in Fig. 2(b) is fitted well with the CI calculation for a $Mn^{3+}(3d^4)$ ion. For the $3d^4$ configuration, the tetragonal distortion of MnO_6 octahedra occurs and splits the energies of e_g and t_{2g} orbitals, as shown in Fig. 3. The energy splitting between $d_{x^2-y^2}$ and d_{z^2} corresponds to the Jahn-Teller (JT) splitting, Δ_{JT}. Our fitting yields $\Delta_{JT}=1.05$ eV for $x=0.3$. This value is in agreement with the known value of ~0.9 eV for $LaMnO_3(Mn^{3+})$, which is obtained from both LDA+U calculation[25] and experimental spectral ellipsometry.[26,27] It should be noted that it was not possible to describe the spectral feature with the CI calculations for the O_h symmetry with nearly all kinds of fitting parameters. Only by lowering the symmetry group of MnO_6 from O_h to D_{4h}, the experimental XAS spectrum could be reproduced, as shown in Fig. 2(b) with the solid line (D_{4h}) and the dotted line (O_h). For $x=0.3$, 10 Dq=1.5 eV and $J=0.9$ eV ($J_{eff}=3J=2.7$ eV$>$10 Dq) imply that the system is in the HS Mn^{3+} state.

The fitting result for the Mn^{4+} calculation for $SrMnO_3$ is shown in Fig. 2(a). The agreement for Mn^{4+} is not as good as for the cases of Mn^{2+} and Mn^{3+}. For $SrMnO_3$, a substantial amount of hybridization between O $2p$ and Mn $3d$ orbitals is predicted, as presented in Table I. All $3d$ electrons for $3d^3$ configuration of Mn^{4+} are in the $t_{2g}\uparrow$ orbitals having the HS state, while the transferred electron from the ligand $2p$ orbitals will be in the $e_g\uparrow$ orbitals.

The increasing 10 Dq in Table I is attributed to the increasing Mn valency. As the Mn valency increases, the

TABLE I. Atomic, crystal-field, and charge transfer parameters used for the fit of the experimental XAS spectra, and the resulting ground-state (GS) configurations. The reduction ratios for the $2p$-$3d(F_{pd})$ and $3d$-$3d(F_{dd})$ Coulomb interactions, 10 Dq: the crystal-field strength, Δ_{JT}: the Jahn-Teller splitting, Δ: the charge-transfer energy, and $V_{pd\sigma}$: the hopping parameter strength.

	F_{pd} (%)	F_{dd} (%)	10 Dq (eV)	Δ_{JT} (eV)	Δ (eV)	$V_{pd\sigma}$ (eV)	GS configuration
Mn^{2+}	80	80	0.9		6.0	1.2	$3d^5(86\%)+3d^6\underline{L}(14\%)$
Mn^{3+}	80	60	1.5	1.05	2.5	1.8	$3d^4(76\%)+3d^5\underline{L}(24\%)$
Mn^{4+}	85	85	2.6		0.0	1.5	$3d^3(45\%)+3d^4\underline{L}(55\%)$

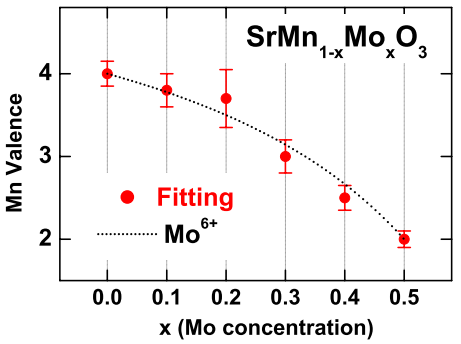

FIG. 4. (Color online) Plots of the valence states of Mn ions in $SrMn_{1-x}Mo_xO_3$ for $0 \leq x \leq 0.5$. Red dots represent the valence states estimated from the CI cluster calculations (see Fig. 2 and Table I), and the dotted line represents the estimated values when all the substituted Mo ions are assumed to be hexavalent (Mo^{6+}).

Mn-O distance ($d_{\text{Mn-O}}$) is shrunk so as to increase 10 Dq. The experimentally obtained $d_{\text{Mn-O}}$'s for $SrMnO_3$ (Ref. 4) and Sr_2MnMoO_6 (Ref. 7) are 1.9 and 2.1 Å, respectively, supporting this argument.

Figures 2(d)–2(f) show the fitting results for the Mn $2p$ XAS spectra for $x=0.1$, $x=0.2$, and $x=0.4$ in $SrMn_{1-x}Mo_xO_3$. These data were fitted by making a linear combination of the calculated Mn^{4+}, Mn^{3+}, and Mn^{2+} XAS in Figs. 2(a)–2(c), respectively, and by varying the relative weights among them. The valence states of Mn ions, estimated from these fittings, are summarized in Fig. 4, which shows the plots of the valence states of Mn ions in $SrMn_{1-x}Mo_xO_3$ for $0 \leq x \leq 0.5$ (red dots). The trend of the decreasing valence states of Mn ions with increasing x in $SrMn_{1-x}Mo_xO_3$ provides evidence that Mo ions are certainly at higher valence states than being tetravalent (4+). The dotted line represents the expected Mn valences when all the substituted Mo ions are assumed to be hexavalent (Mo^{6+}). This comparison reveals a reasonably good agreement between the fitting results (red dots) and the expected values for Mo^{6+} ions (dotted line). This finding indicates that Mo ions in $SrMn_{1-x}Mo_xO_3$ are close to being hexavalent (Mo^{6+}) for $x \leq 0.5$.

Figure 5(a) shows the Mo $3p$ XAS spectra of $SrMn_{1-x}Mo_xO_3$ $(0 \leq x \leq 0.5)$. Even though the quality of the measured XAS data is not good, the peak positions and the lineshapes of the Mo $3p$ XAS spectra do not change with x. This finding again reflects that the valence states of Mo ions in $SrMn_{1-x}Mo_xO_3$ do not change with x. Figure 5(b) compares the Mo $3d$ core-level photoemission spectroscopy (PES) spectra of $SrMn_{1-x}Mo_xO_3$ $(0 \leq x \leq 0.5)$ to those of reference oxides of MoO_3 and Sr_2FeMoO_6. The Mo $3d$ PES spectra of $SrMn_{1-x}Mo_xO_3$ were obtained from scraped samples at room temperature by using the monochromatized Al source. MoO_3 is taken from Ref. 28 and is chosen as a formally hexavalent (Mo^{6+}) system, while Sr_2FeMoO_6 (our data) is shown as a Mo^{5+}-Mo^{6+} mixed-valent system.[29] Note

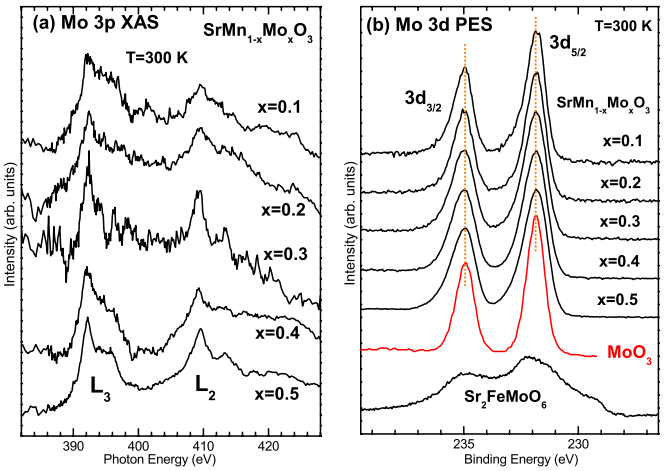

FIG. 5. (Color online) (a) Comparison of the Mo $3p$ XAS spectra of $SrMn_{1-x}Mo_xO_3$ $(0 \leq x \leq 0.5)$. (b) Comparison of the Mo $3d$ PES spectra of $SrMn_{1-x}Mo_xO_3$ $(0 \leq x \leq 0.5)$ to those of reference oxides of MoO_3 and Sr_2FeMoO_6.

that the Mo $3d$ PES spectrum of Sr_2FeMoO_6 exhibits several peaks and is much broader than that of MoO_3, reflecting its mixed-valent and metallic ground state. This comparison shows clearly that the Mo $3d$ PES spectra of $SrMn_{1-x}Mo_xO_3$ are very similar to each other in both the peak positions and the lineshapes, which confirms that the valence states of Mo ions do not change with x. Further, the peak positions and the lineshapes of the Mo $3d$ PES spectra of $SrMn_{1-x}Mo_xO_3$ are very similar to that of MoO_3, but quite different from that of Sr_2FeMoO_6, indicating that the valence states of Mo ions in $SrMn_{1-x}Mo_xO_3$ are close to being hexavalent.

IV. CONCLUSION

We have studied the electronic structures of $SrMn_{1-x}Mo_xO_3$ $(0 \leq x \leq 0.5)$ by employing Mn $2p$ XAS and the subsequent CI cluster model analyses. We have found that, due to the substitution of hexavalent $Mo^{6+}(4d^0)$ ions, the valence states of Mn ions change systematically with increasing x, from HS Mn^{4+} for $x=0$, to nearly HS $Mn^{3+}(t_{2g}^3\uparrow e_g^1\uparrow)$ for $x=0.3$, and HS Mn^{2+} ions $(t_{2g}^3\uparrow e_g^2\uparrow)$ for $x=0.5$. The Mn $2p$ XAS spectra are described very well with the CI cluster calculations including the JT effect for Mn^{3+} ions, which confirms the systematic change in the Mn valence state in $SrMn_{1-x}Mo_xO_3$ for $0 \leq x \leq 0.5$.

ACKNOWLEDGMENTS

This work was supported by the NRF under Contracts No. 2009-0079947 and No. 2009-0064246, and in part by the 2009 Research Fund of the CUK. The experiment at PLS is supported by POSTECH and MOST. Work at NIU was supported by the NSF (Grant No. DMR-0706610).

*Corresponding author; kangjs@catholic.ac.kr

[1] J. M. D. Coey, M. Viret, and S. Von Molnár, Adv. Phys. **48**, 167 (1999).
[2] K.-I. Kobayashi, T. Kimura, H. Sawada, K. Terakura, and Y. Tokura, Nature (London) **395**, 677 (1998).
[3] K. Kikuchi, H. Chiba, M. Kikuchi, and Y. Syono, J. Solid State Chem. **146**, 1 (1999).
[4] O. Chmaissem, B. Dabrowski, S. Kolesnik, J. Mais, D. E. Brown, R. Kruk, P. Prior, B. Pyles, and J. D. Jorgensen, Phys. Rev. B **64**, 134412 (2001).
[5] Rune Søndenå, P. Ravindran, Svein Stølen, Tor Grande, and Michael Hanfland, Phys. Rev. B **74**, 144102 (2006).
[6] M. Itoh, I. Ohota, and Y. Inaguma, Mater. Sci. Eng., B **41**, 55 (1996).
[7] A. Muñoz, J. A. Alonso, M. T. Casais, M. J. Martínez-Lope, and M. T. Fernández-Díaz, J. Phys.: Condens. Matter **14**, 8817 (2002).
[8] I. V. Solovyev, J. Magn. Magn. Mater. **268**, 194 (2004).
[9] Y. Moritomo, Sh. Xu, A. Machida, T. Akimoto, E. Nishibori, M. Takata, and M. Sakata, Phys. Rev. B **61**, R7827 (2000).
[10] W. J. Lu, Y. P. Sun, B. C. Zhao, X. B. Zhu, and W. H. Song, Phys. Rev. B **73**, 174425 (2006).
[11] B. Raveau, Y. M. Zhao, C. Martin, M. Hervieu, and A. Maignan, J. Solid State Chem. **149**, 203 (2000).
[12] L. Pi, S. Hébert, C. Martin, A. Maignan, and B. Raveau, Phys. Rev. B **67**, 024430 (2003).
[13] S. B. Zhang, Y. P. Sun, B. C. Zhao, X. Luo, C. Y. Hao, X. B. Zhu, and W. H. Song, J. Appl. Phys. **102**, 103903 (2007).
[14] B. Dabrowski, O. Chmaissem, J. Mais, S. Kolesnik, J. D. Jorgensen, and S. Short, J. Solid State Chem. **170**, 154 (2003).
[15] The XAS spectra, obtained at room temperature and at $T \sim 80$ K, were essentially the same.
[16] T. Burnus, Z. Hu, H. H. Hsieh, V. L. J. Joly, P. A. Joy, M. W. Haverkort, Hua Wu, A. Tanaka, H.-J. Lin, C. T. Chen, and L. H. Tjeng, Phys. Rev. B **77**, 125124 (2008).
[17] Our data.
[18] P. Ghigna, A. Campana, A. Lascialfari, A. Caneschi, D. Gatteschi, A. Tagliaferri, and F. Borgatti, Phys. Rev. B **64**, 132413 (2001).
[19] C. Mitra, Z. Hu, P. Raychaudhuri, S. Wirth, S. I. Csiszar, H. H. Hsieh, H.-J. Lin, C. T. Chen, and L. H. Tjeng, Phys. Rev. B **67**, 092404 (2003).
[20] The program used in this work is TT multiplet, which was provided by de Groot.
[21] W. A. Harrison, *Electronic Structures and Physical Properties of Solids* (Freeman, San Francisco, 1980).
[22] A. E. Bocquet, T. Mizokawa, K. Morikawa, A. Fujimori, S. R. Barman, K. Maiti, D. D. Sarma, Y. Tokura, and M. Onoda, Phys. Rev. B **53**, 1161 (1996).
[23] F. M. F. de Groot, Coord. Chem. Rev. **249**, 31 (2005).
[24] Different values of 2γ are applied to the L_3 and L_2 part separately, with the ratio of $L_3:L_2 \sim 1:1.5$ and $2\gamma(L_3) \approx 0.3$ eV.
[25] W.-G. Yin, D. Volja, and W. Ku, Phys. Rev. Lett. **96**, 116405 (2006).
[26] N. N. Kovaleva, A. V. Boris, C. Bernhard, A. Kulakov, A. Pimenov, A. M. Balbashov, G. Khaliullin, and B. Keimer, Phys. Rev. Lett. **93**, 147204 (2004).
[27] R. Rauer, M. Rübhausen, and K. Dörr, Phys. Rev. B **73**, 092402 (2006).
[28] M. Sing, R. Neudert, H. von Lips, M. S. Golden, M. Knupfer, J. Fink, R. Claessen, J. Mücke, H. Schmitt, S. Hüfner, B. Lommel, W. Assmus, Ch. Jung, and C. Hellwig, Phys. Rev. B **60**, 8559 (1999).
[29] J. H. Kim, S. C. Wi, S. Yoon, B. J. Suh, J.-S. Kang, S. W. Han, K. H. Kim, A. Sekiyama, S. Kasai, S. Suga, C. G. Olson, B. J. Park, and B. W. Lee, J. Korean Phys. Soc. **43**, 416 (2003). The Mo $3d$ PES spectrum for Sr_2FeMoO_6 was obtained with $h\nu = 704$ eV at $T \sim 20$ K.